A visual analytics perspective on shape analysis: state of the art and future prospects

Max Hermann   Reinhard Klein

Institute of Computer Science II, University of Bonn, Germany

Abstract

The combination of long established techniques in morphometrics with novel shape modeling approaches in geometry processing has opened new ways of visualizations of shape variability in different application areas like biology, medicine, epidemiology and agriculture. For the first time highly resolved 3D representations became accessible for statistical analysis as well as visualizations. In order to reveal causes for shape variability targeted statistical analysis correlating shape features against external and internal factors is necessary but due to the complexity of the problem often not feasible in an automated way. Therefore, visual analytics methods found their way into the field of morphometrics. This led to numerous publications in recent years that might be subsumed under the novel term visual shape analytics. In this paper we try to put these works into the context of visual analytics, outline the basic principles underlying these approaches and review the current state of the art. Finally, future challenges and possibilities in visual shape analytics are identified.

Keywords: Shape analysis, visual analytics, visual shape analytics, shape space, visualization

1. Introduction

In morphometrics and its application fields like medicine or biology experts are interested in causal relations of organismic shape to phylogenetic, ecological, geographical or epidemiological factors. In order to assist experts in getting *insight* into the variability of shapes and uncover potential sources a variety of different visual analytics methods for shape analysis has emerged in recent years that might be subsumed under the novel term *visual shape analytics*. These methods do not aim at a fully automated statistical analysis but instead rather provide interactive tools for an effective exploration of shape variation. This is achieved by means of interactive visualizations in order to stimulate quick hypothesis generation and feature assessment.

The visualizations used frequently during morphometric studies so far, were designed primarily for the purpose of communicating final results of a statistical analysis [21, 56]. Only recently the potential of an interactive approach for exploration of shape spaces has been recognized and targeted analysis tools, especially for population studies that deal with large data collections were developed [20, 42, 53, 44] and as outlined by Botha et al. [17] further research is needed to come up with novel techniques to exhibit the complex correlations between shape variability and extrinsic as well as intrinsic factors.

In this paper it is shown that the combination of methods from interactive computer graphics and visualization with methods from statistical shape analysis deliver novel ways to investigate and explore complex morphological inter-dependencies. Both domains have a long tradition at the IGD where not only interactive computer graphics techniques and visualization were early in the focus of research [72] and statistical shape models are extensively utilized in the context of medical image analysis until today [52]. Recently, a first Visual analytics approach to provide a better understanding of the impact of particular optimization algorithms for medical image segmentation and their parameters on a local scale were introduced by Landesberger et al. who continued this long tradition at the IGD [89].

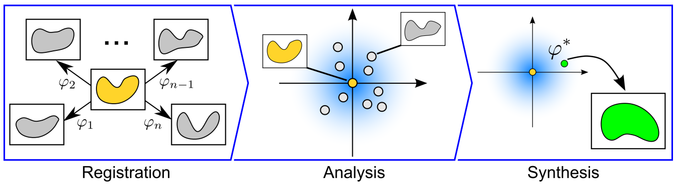

Figure 1: The modeling pipeline for visual shape analytics.

By reviewing the state of the art in modeling, navigation and visualization of shape spaces we summarize the current methods and identify new trends in this emerging field.

2. The visual analytics approach to shape analysis

As already stated by Daniel Keim et al. [47] in their work about the foundation of visual analytics, *Visual Analytics combines automated analysis techniques with interactive visualizations for an effective understanding, reasoning and decision making on the basis of very large and complex data sets*. The major task of visual shape analytics consists in linking abstract representations of the high dimensional shape space with a corresponding 3D visualization in such a way that an effective *navigation* in shape space is enabled. This requires efficient automatic analysis techniques as well as real-time sampling in shape space and 3D visualizations.

Initially, this idea of navigating shape spaces was brought forward in the work of Busking et al. [20], although they ex-

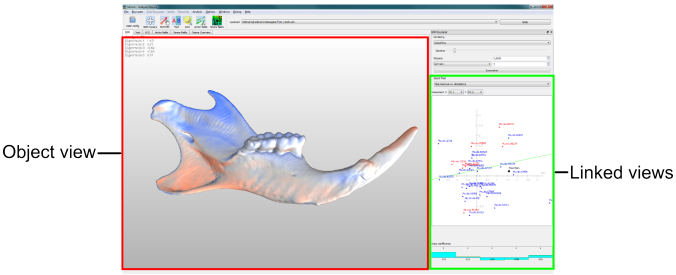

Figure 2: The user interface of a visual shape analytics system is usually split into a 3D object view that provides different visualizations of shape variability and linked abstract views like the shown interactive scatter plot.

cluded any automated analysis. They present a manual navigation in the abstract representation of the shape space that is presented as a scatter plot in a 2D projection of a linear shape space. The selection of a position in the scatter plot triggers the sampling of a shape in the linear shape space by interpolation of the adjacent shapes that are identified in the two dimensional domain. Although the individual techniques were improved later on, their work already outlines the general visual analytics approach, see figure 1. In a first step shape variability is represented by registration of the individual shapes of the shape ensemble against a template which often coincides with their mean shape [37]. Based on this registration the individual shapes are represented by the transformation that deforms the template into the particular shape. After applying statistical analysis on the deformations novel samples are synthesized and can be visualized on demand. In the end this facilitates *navigation* in shape space, that is, sampling shapes at particular points, along any direction or even arbitrary trajectories in abstract data space. This *synthesis* of deformation provides the basic exploration facility of the visual analytics approach and therefore also must be real-time in order to allow interactive exploration. The crucial aspect of visual analytics in this general setting is to support the user in intelligent navigation in shape space and to apply further statistical analysis when needed. This way a feedback loop between statistical analysis and visualization is established. Following the visualization mantra "overview, zoom & filter, then details-on-demand" [77] methods targeting different levels of abstraction were developed, see table 1. All of the methods can be used in combination, enabling the user to drill down into sub spaces of shape space for a targeted analysis of particular local or global aspects of shape variation.

Special care has to be taken to design a user interface accessible to the domain experts. An example of such an user interface is shown in figure 2.

3. Modeling of shape and its variation

A mathematical definition of shape was given by David G. Kendall [48] who puts it as the idea *to filter out effects resulting from translations, changes of scale and rotations and declare that shape is "what is left"*. This does not only apply to surface and point data that is usually associated with the term shape, but also to the volumetric structure of an anatomy as represented in biomedical images. In contrast to landmark and surface representations the volumetric representation has the advantage that the internal structures are included in the analysis.

3.1. Representation of shape difference

Before the statistical analysis of variation, at least rigid transformations, i.e. translation and rotation, are factored out because position and orientation are arbitrary, depending solely on the choice of some external coordinate frame. Sometimes the class of rigid motions is extended to similarity transformations, including isotropic scaling, or even to the fully affine case, depending on the study at hand. After filtering out these affine transformations the remaining difference in shape is subsequently considered as the shape variation of interest. The remaining difference between the shapes is captured by non-rigid deformations that establish dense correspondences between each shape and a template. In general the template itself is found during the computation of correspondences [93, 28].

As a consequence of these considerations, whenever comparing two shapes via a transformation φ that maps one shape onto the other, φ is decomposed into two parts

$$\varphi = \varphi_{\text{global}} \circ \varphi_{\text{local}}. \tag{1}$$

The global part φ_{global} accounts for non-shape differences and will be realized by a linear transformation as discussed. When comparing an ensemble of shapes against some template shape, all global parts will be factored out first in a preprocessing step. The particular procedure to do this is referred to as *alignment*. Thereby a common coordinate frame between the anatomies of an ensemble is established, i.e. the one of the template. After the alignment procedure, the remaining local parts φ_{local} are pivotal to further analysis, as they represent the shape variation of the ensemble. In summary, one can say that φ_{global} defines what shape is, while φ_{local} encodes shape difference and variation.

The transformation φ_{local} is parametrized via a displacement vector field $u(x)$

$$\varphi_{local}(x) = x + u(x). \tag{2}$$

that is computed via deformable image registration methods, see e.g. [81]. Very popular and successful in image registration are physics-based deformation models [65] which comprise diffusion based approaches including elastic body and viscous fluid flow models [33]. Also from this class are flows of diffeomorphisms that are implemented in the framework of large displacement diffeomorphic metric mappings (LDDMM) [9]. These are prominently introduced in computational anatomy and are especially suited to study anatomical variability [63] especially in the case of large deformations [24]. Unfortunately, synthesis in LDDMM requires computationally very expensive algorithms like geodesic shooting [64], which are out of reach for interactive applications in the foreseeable future. A very promising alternative representation based on stationary velocity fields (SVF) emerged recently [4, 5]. This method allows for efficient visualizations [44]. Alternative methods originated from interpolation theory. In contrast to the above displacement representation, these approaches are parametrized over

Sec.	Method		Purpose
4.1	Regression [13, 2]	(f)	Define a direction in PCA space that parametrizes a labeled attribute.
4.1	Classification [42]	(d)	Define a direction in PCA space corresponding to the characteristic shape difference between two groups.
4.1	Likelihood volume [21]	(o)	Integrated visualization of direction in PCA space, e.g. overview of principal modes.
4.2	Scatter plot [20]	(d)	Manual navigation in PCA space by specifying sample shapes via selecting positions in a scatter plot view.
4.2	Barycentric coordinates [80]	(d)	Manual navigation in shape space by specifying a linear combination as generalized barycentric coordinate of a clicked point in a 2D convex polygon whose vertices represent the sample shapes.
4.3	Interaction tensor [43]	(f)	Targeted analysis of covariation between points on the shape, e.g. to identify hypotheses on module limits.
4.3	Model based editing [12]	(d)	Targeted analysis of covariation between points on the shape with respect to specific perturbation.
4.3	Region of interest [42]	(f)	Define a PCA space w.r.t. a selected ROI to focus investigation on particular local structures.
4.4	Group browser [44]	(f)	Comparative visualization of multiple factors by interpolating between group mean shapes.

Table 1: List of methods to navigate shape spaces, classified according to Shneiderman [77] into (o) overview, (f) focus and (d) detail view.

interpolating functions that provide a more compact representation amenable to efficient optimization schemes. Important examples are free form deformations (FFD) and thin plate spline (TPS) interpolation. For FFD the deformation is represented as low-degree B-splines on a coarse control grid [8, 74]. Rueckert et al. [71] introduced statistical deformation models based on FFD by applying PCA to the B-spline coefficients. TPS interpolate smoothly between given control points by minimizing bending energy [90] and are thereby a suitable way to augment the result of a landmark analysis to the space in between landmarks for visualization purposes. Drawbacks of the parametric TPS and FFD approaches are, that they are not inherently diffeomorphic. FFD easily produces self-overlaps while TPS interpolation often yields implausible deformations away from its control points. Further, both methods provide only a limited resolution determined by the grid size in FFD and control point placement in TPS.

3.2. *Statistical deformation model*

The variability contained in a shape ensemble can be described using first and second order moments, i.e. mean and covariance of the displacement vector field u. The analysis of this vector field can be reduced to multivariate statistics by treating each voxel and each dimension separately. For this purpose it is convenient to consider the vector field as a long column vector $\mathbf{u} \in \mathbb{R}^{3N}$ where N denotes the number of voxels in the discretized image domain Ω.

Based on the concept of linearity, the first moment is found as the arithmetic average

$$\bar{\mathbf{u}} = \frac{1}{n}\sum_{i=1}^{n}\mathbf{u}_i. \tag{3}$$

If the template shape coincides with the mean shape then $\bar{\mathbf{u}} = 0$ and the displacement fields constitute the data matrix $\mathbf{X} = [\mathbf{u}_1, \ldots, \mathbf{u}_n] \in \mathbb{R}^{3N\times n}$. From this, the second moment is estimated as the $3N \times 3N$ sample covariance matrix $\mathbf{\Sigma} = \frac{1}{n-1}\mathbf{X}\mathbf{X}^T$. In order to ease interpretation of covariance, a principal component analysis (PCA) is performed that provides an uncorrelated basis $\mathbf{B}$ of dimension $n' \leq n-1$ in which the covariance matrix becomes diagonal. Note that each column vector of $\mathbf{B}$ represents itself a deformation encoded as displacement vector field and is termed *mode of (shape) variation*. Taking linear combinations of these modes constitutes a generative model

$$\mathbf{u} = \mathbf{B}\mathbf{c} \tag{4}$$

where $\mathbf{c} = (c_1, \ldots, c_{n'})^T$ should be chosen with $c_i \in [-3, +3]$ conforming to a range of three standard deviations σ_i of the underlying normal distribution model:

$$p(\mathbf{c}) = (2\pi)^{-n'/2}\, e^{-\frac{1}{2}\|\mathbf{c}\|^2}.$$

An important drawback of models derived by PCA is inherent dependency of the result on the L^2- metric, which favors low frequency changes of the shape that corresponds to global shape variations but neglect subtle details whose shape variations is often spread over several modes. In order to overcome this problem locally weighted PCA can be applied [42].

While the above linear model of the shape space is sufficient for small displacements, i.e. if $\|u(x)\|$ is small, which holds for example for most genetic studies, it fails to describe larger variabilities among a population, that in biology for example are caused by ecological factors. In this case the underlying linear shape space and the linear mean (3) is replaced by considering the non-linear manifold of diffeomorphisms and the Fréchet mean. For a smooth manifold X endowed with a metric d, the Fréchet mean of a set $\{x_1, \ldots, x_n\}, x_i \in X$, if it exists and is unique, is defined as

$$\bar{x} := \arg\min_{x^*} \frac{1}{n}\sum_{i=1}^{n} d(x_i, x^*)^2. \tag{5}$$

In order to compute the Fréchet mean, several group-wise registration approaches have been developed [38, 6, 46] by defining a suitable metric on the space of deformations based on (5). Starting from a candidate image, the general concept is to iteratively update this image such that the average of squared geodesic distances between template and each individual approaches a minimum. In the context of geometric modeling custom designed metrics in the space of linear transformations was introduced by Alexa [1] and later on generalized by Kilian et al. [49] to as-isometric-as-possible deformations between registered 3D meshes. Unfortunately, the calculation of geodesic distances is computationally expensive and in general not possible in real-time [64]. A compromise is restricting the space of diffeomorphisms to the ones that are generated by SVFs as suggested by Arsigny et al. [4]. While in the LDDMM framework [9] a diffeomorphic mapping φ is constructed as the endpoint $\varphi = \Phi_1$ of the flow of a time-varying velocity field $v_t : \Omega \longrightarrow \mathbb{R}^n, t \in [0, 1]$ specified by

$$\frac{d}{dt}\Phi_t = v_t(\Phi_t) \tag{6}$$

leading to a path $\Phi_t : \Omega \longrightarrow \Omega, t \in [0, 1]$ in the tangent space of the Riemannian manifold of diffeomorphisms starting with $\Phi_0 = Id$ and terminating at the endpoint

$$\varphi := \Phi_1 = \Phi_0 + \int_0^1 v_t(\Phi_t)dt \tag{7}$$

matching the given image, the restriction to a stationary flow $v_t = v$ simplifies the integration tremendously while still being sufficiently expressive to describe large deformations as demonstrated by successfully modeling the variability of a range of different anatomies [5, 16, 76]. Even more important, in the case of SVFs the resulting family of flows $\Phi_t, t \in [0, 1]$ is a one-parameter subgroup of diffeomorphims with infinitisimal generator v. By defining the exponential map of a stationary vectorfield v as the diffeomorphism obtaind by

$$\exp(v)(x) := \varphi(x) = \Phi_1(x) = \Phi_0(x) + \int_0^1 v(\Phi_t(x))dt\,, \tag{8}$$

the logarithm $\log(\varphi)$ of a diffeomorphism φ close enough to identity is the unique vector field v in a neighborhood of zero such that $\exp(v) = \varphi$. Of special interest for visual shape analytics and a key advantage of this approach is that it allows for *log-euclidean statistics* on diffeomorphisms. The log-domain, where velocity fields live, offers a natural linearization

$$\varphi_a \circ \varphi_b = \exp(v_a) \circ \exp(v_b) = \exp(v_a + v_b) \tag{9}$$

that is lifted to the diffeomorphic group structure by integration, i.e, on the log-space of diffeomorphisms one can perform Euclidean operations. As a direct consequence the average $\bar{\varphi}$ of a set of deformations $\{\varphi_1, \ldots, \varphi_n\}$ can be computed as

$$\bar{\varphi} = \exp(\bar{v}) \quad \text{with} \quad \bar{v} = \frac{1}{n}\sum_{i=1}^{n} v_i \quad \text{where} \quad v_i = \log(\varphi_i) \tag{10}$$

and the same linear PCA statistics as described above can be applied on the set $\{v_i\}$ of logarithms resulting in a generative model

$$\mathbf{v}_{\hat{c}} = \hat{\mathbf{B}}\hat{\mathbf{c}} \tag{11}$$

with a basis matrix $\hat{\mathbf{B}}$ of principal velocities. Note, that in applications the logarithm is often provided by the registration algorithm.

4. Navigation in shape space

A particular focus of application of shape space representations in computer graphics is effective authoring of 3D content by means of interpolation in available 3D model databases, see [13, 2, 3] to cite just a few works in this field. In computer vision [26, 18] and medical image segmentation [41] shape space representations are used to introduce model knowledge. A special advantage in all these works is their combination of statistical analysis and efficient synthesis to generate novel 3D shapes that are plausible w.r.t. a statistical model. This is exactly what is necessary for interactive visual exploration of shape variability in the context of visual shape analytics. However, in order to enable *targeted exploration* of a shape ensemble additional methods for navigation in shape space are required. A key challenge in this context is to make the high dimensionality of shape spaces accessible.

4.1. Navigation along traits

A first idea on this was already given by Blanz and Vetter [13] who parametrized the shape of human faces via regression on semantically motivated traits like age, sex, weight, etc. in PCA space. They demonstrated that exaggerating these traits can be used to create easily understandable caricatures of certain type. Matusik et al. [62] showed that navigation along traits is an effective means of identifying specific characteristics in the context of reflectance functions. In the context of visual shape analytics this idea was applied to relate shape variation to external attributes by Hermann et al. [42]. In this work trait vectors in shape space are derived interactively from external attributes by training a support vector machine. Navigating along the resulting trait vector is simultaneously visualized in a two-dimensional scatter plot and a 3D-object view that shows the corresponding variation as a deformation of the template.

4.2. Navigation via scatter plots

Manual exploration using two dimensional views as interfaces for navigation were suggested by several authors. Kilian et al. [49] present a shape exploration based on barycentric interpolation between example shapes. To this end a 2D embedding view of the shape ensemble is derived via multidimensional scaling (MDS) followed by a triangulation. By drawing curves in this view, arbitrary interpolations can be explored. Instead of a triangulation, Smith et al. [80] rely on generalized barycentric interpolation inside a convex control polygon that, by clicking a point inside the polygon, allows the user to dial up a particular affine combination of a set of registered car shape models. Additional regression values on specific attributes like *sportiness* are overlaid on the polygon for guidance. For the specific case of mesh animations, Cashman et al. [22] use a combination of MDS and radial basis functions to come up with a 2D map visualization of the animation as a spline curve. On this map, a repetitive motion will for instance show up as a curve with several loops. By manipulating the curve, the animation can be edited in a high level way. Busking et al. [20] use a scatter plot that shows a 2D projection of PCA space. The projection can be adjusted interactively by manipulating 2D representations of a set of axes or vectors in shape space [11]. For synthesis of shapes in-between sample points in the 2D projection natural neighbors interpolation is used, based on a Voronoi tessellation that is computed efficiently on the GPU. Klemm et al. [53] use multiple linked views to explore medical population data for epidemiology, e.g. to identify disease-specific risk factors. Aim of their interactive visual analysis is parameter and group selection for subsequent statistical analysis. The data also includes MR images from which 3D surface models of the lumbar spine are semi-automatically extracted. During exploration, mean shapes of selected groups are displayed while their color encodes the difference to the global mean shape.

4.3. *Direct manipulation approaches*

An interesting alternative to interaction with abstract 2D views and scatter plots are direct manipulation approaches to explore and generate shape variations. Probably one of the first approaches in this regard is model based editing introduced by Blanz et al. [12]. Based on the user modifying the position of just a few feature points their approach optimizes the most likely shape that matches the user input as closely as possible. Thanks to the linearity of the PCA model this optimization turns out to be a simple least squares problem that can be solved efficiently. Lewis and Anjyo [59] pick up the same idea for editing facial blendshape models while Tena et al. [82] and Berner et al. [10] present generalizations of this approach to part based shape models. Coffey et al. [25] present an interactive manipulation interface to navigate the space of simulation outputs in order to refine the design of a mechanical biopsy device, taking into account its functionality. Interestingly, the metaphor of direct spatial manipulation has been recently applied also to time-varying scatter plots [57], where dragging around a point facilitates navigation in time by matching the input to an existing point and its temporal trajectory. Hermann et al. [43] used the model based deformation to analyze covariance on shapes. The basic idea of their approach is to reinterpret and extend the model based editing introduced by Blanz et al. to either observe the shape change correlated to the perturbation of a single point that is dragged by the user or to perform a covariance analysis between possible edits at a single point and its impact on other points on the surface. The single point edit nicely uncovers the dependency of shape variability on directional changes of a certain structure as shown in figure 3. The covariance analysis between the edit at a single point and its impact on the rest of the shape is summarized by two alternative methods, see figures 3 and 4. First, the effect on a point q of a perturbation of unit size towards arbitrary directions at a point p is captured at the point q by the covariance matrix of the corresponding changes at q. Second, to summarize the possible influence of perturbations of a point p this covariance structure is integrated over the remaining positions leading to a covariance matrix that indicates both, strength and its dependence on direction of perturbations of p. All three methods are of special interest in the biological context of modularity and integration. This relates to partitioning a shape into modules such that the perturbations inside a module are integrated, but are relatively independent from other modules [54]. Integration here refers to the degree that particular shape characteristics depend on each other, see figure 4.

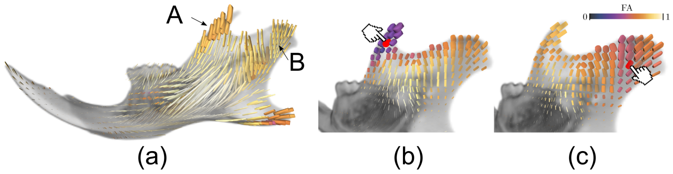

Figure 3: Covariance tensor visualization of Hermann et al. [43]. **(a)** An overview guides the expert to points that exhibit interesting covariation. **(b,c)** Covariation analysis of the impact of perturbation at a particular point into arbitrary directions reveals the associated covariation patterns.

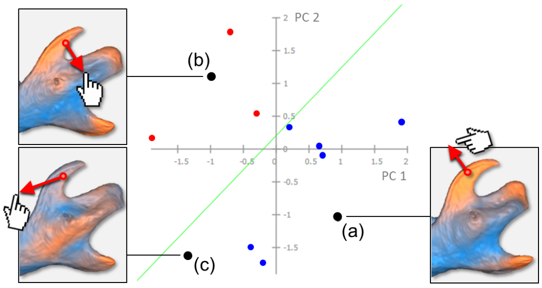

Figure 4: Model based editing allows to investigate shape covariation depending on a perturbation of a single point on the shape into specifc directions [43]. This assists in identifying integrated modules of the shape, i.e. parts on the shape that exhibit strongly correlated shape changes (see text).

4.4. *Navigation of subensembles*

For industrial CT images comparative visualizations were made for the analysis of defects for material sciences [69]. In order to visualize the shape distribution of a set of feature objects, pores or other material defects in form of an uncertainty cloud the concept of mean objects was introduced. Clustering of mean objects provides a hierarchical representation well suited for exploration. A key difference to navigation in shape space where the dense registration between the individual shapes is crucial, the defects need only to be coarsely aligned.

A common task for exploratory morphometric analysis is to disentangle the factors that determine shape variation. This was achieved by Hermann et al. [44]. In this work categorical factors decompose the shape ensemble into subsets, for instance into several phylogenetic or dietary groups. In order to unveil the impact of each factor on shape variation, mean shapes of the corresponding subsets are derived on the fly, enabling interpolation in-between group means and the ensemble template. An example of browsing group means is given in figure 5.

5. Visualization of shape variability

Although visualization plays such a central role in shape analysis, there seem to be only two articles published yet that give sort of a survey [56, 21]. Klingenberg [55] critically discusses common visualization methods for landmark analyses in geometric morphometrics and provides helpful guidelines for practitioners. Different visualization options for statistical deformation models used in computational anatomy are compared by Caban et al. [21] and evaluated in a small user study. Both works contribute valuable insights about effectiveness and limitations of many important visualization techniques. However,

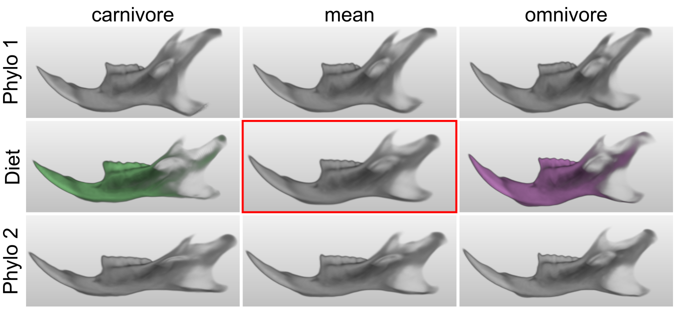

Figure 5: Browsing mean shapes of different groups related to extrinsic factors like phylogeny and diet in this example allows comparative analysis of the impact of these factors onto anatomy [44]. The ensemble mean is highlighted. ©2015 IEEE. Reprinted, with permission.

some often encountered visualizations such as color coded isosurfaces or vector fields are missing in the mentioned surveys, and animation is not discussed either. Therefore a structured presentation of available techniques including the previously left-out ones seems in order.

5.1. Taxonomy and review of visualization techniques

Visualization techniques can be grouped by their primary underlying visual paradigm: *Superimposition* and *side-by-side comparison* relate to spatial layout, *direct visualization* focuses on ways to display deformation by warping methods, *encoded visualization* is about the use of color-coding and glyphs to communicate higher order information and finally, *animation* deals with the temporal dimension.

Superimposition. The original shape samples are shown superimposed in a reference coordinate system, e.g. given by Procrustes alignment. This kind of display is quite common and effective for 2D landmark and contour data [56] and is used in many publications and textbooks in geometric morphometrics. An advantage is, that it does not require a deformation or statistical model per se. Nevertheless, plotting for instance superimposed landmarks yields point clouds whose distributions reveal the local covariance structure at each landmark. Superimposing contour data gives a good overview of global variability but quickly becomes cluttered for many contours. In our experience, this cluttering becomes even worse when superimposing 3D surfaces [7], because of the additional occlusion interfering with the superimposition. In practice we observe that at most three surfaces are shown superimposed using alpha blending and contrasting colors, see e.g. RegistrationShop [79]. Superimposition is also used to assess results of pairwise registration of surfaces or images. The interactive 3D volume registration system of Smit et al. [79] makes use of multi-volume rendering to superimpose fixed and moving volume, color-coded and opacity blended to reveal areas of mis-registration. The checkerboard method is an alternative way of superimposition of two 2D images (or slices of a volume) that does not require blending. The white squares of the checkerboard offer a view onto one of the images, the black squares onto the other. A generalization of this technique to more than two images was presented by Malik et al. [61] and a generalization to tensor field visualization was recently given by Zhang et al. [95]. Likelihood volumes [21, 45] can be understood as a generalized superimposition of 3D images by means of blending more than two images. An efficient implementation of a likelihood volume for non-linear deformation model (11) was presented by Hermann et al. [44] where it is used as an overview visualization. When sampling a deformation densely, likelihood volumes produce a visualization resembling motion blur. A similar approach was taken to visualize the uncertainty of estimated isosurfaces [68, 66].

Side-by-side comparison. Instead of superimposing one or more shapes in a single view, multiple views can be employed as well. This provides an alternative in cases where superimposition is not applicable or would lead to a cluttered display. Unfortunately, small scale shape variations are hard to recognize. Following Tufte's small multiples [87], a small-scale shape rendering can serve as an iconic representation that allows comparative displays showing many shapes at once. This technique is used for instance to overlay small shape renderings on a scatter plot showing a 2D projection of shape space [20].

Direct visualization. This paradigm subsumes approaches that depict deformations explicitly by deforming a graphical representation of the shape or the embedding 3D space. Showing a distorted Cartesian grid is amongst the classic methods to illustrate anatomic deformation, as it was already introduced by D'Arcy Thompson [83] and even earlier by Artists like Dürer and Da Vinci in their anatomical studies. While these early examples were hand-crafted, the first automatic graphics procedure was introduced by Bookstein [14] based on thin-plate spline (TPS) interpolation of space in between landmarks. This remains one of the dominant visualizations in morphometrics to this day [56] and can be used to deform grids as well as shape representations. A reason for the popularity of direct space warping techniques is probably that they can be applied to landmark and surface data in 2D or 3D in the exact same manner. Wiley et al. [91] use TPS for instance to interpolate between known sample shapes from an evolutionary tree to generate hypothetical ancestral shapes. Somewhat a hybrid between direct and encoded visualization (see below) are the deformable grids [23, 21]. Initially developed for 2D uncertainty data [23] they were generalized to show anatomic variation from statistical deformation models in 3D by Caban et al. [21]. A very coarse grid is overlaid onto the image and deformation is visualized by modulating the depiction of grid edges, e.g. by drawing an edge as a sinusoid curve with the local deformation magnitude mapped to its amplitude.

Encoded visualization. In contrast to direct visualization, methods that fall under this paradigm visualize particular aspects of deformation implicitly by means of color coding or glyph rendering. Scalar attributes are easily visualized via color coding by applying a transfer function that maps the scalar value range to some color gradient. In computational anatomy one often encounters variability and probability maps that color code magnitude of local variability and outcome of statistical tests respectively [84]. Hamarneh [39] use color coding to show "hot spots" of localized shape variation. Lüthi et al. [60] use color coding to visualize the remaining flexibility of a statistical shape model after parts of it have been fixed, for instance by a semi-automatic model based registration procedure. Zollikofer and Ponce de Léon [96] show a successful combination of color coding and vector field visualization on 3D surfaces to communicate deformation decomposed into directions parallel (vector field) and perpendicular (color) to the surface. Kirschner and Wesarg [51] present an implementation of this kind of visualization in an interactive system for active shape models.

Kindlmann et al. [50] visualize anatomic covariance tensor fields using superquadric tensor glyphs that summarize the local covariance structure at each sample point on the surface of a mean shape. For each point a 3×3 sample covariance matrix on the set of displacement vectors from the mean to each individual is computed. Additional scalar measures derived from the covariance tensor data like fractional anisotropy and Frobenius norm are used for color coding glyphs and shape surface respectively. The same glyph visualization is used for the covariance tensors described in Hermann et al. [43]. Van Golen [88] uses custom glyphs to show the influence of each landmark on an active shape model, i.e. how strongly the overall shape variation described by the model depends on a particular landmark.

When dealing with image based shape models, deformations are often represented as dense vector fields. This enables vector field visualization methods like color coding of Jacobians [70], detection of critical points and display via glyphs [85] or color coding custom tailored scalar flow measures [19]. Streamline rendering is another vector field visualization method [76] that was used by Hermann et al. [44] to uncover the tangential component of non-linear shape variations.

Animation. Showing a particular variation as image deformation in an animated way is an ideal presentation to the human eye [84, 58]. It allows to utilize the excellent motion perception capabilities of humans that renders small deformations much better perceivable than from a set of static images. Therefore, animation is one of the preferred visualizations in many approaches. It is an obvious choice when illustrating dynamic processes like respiratory motion of lungs and inner organs in humans. Handels and Hacker use animation to present an interactive anatomical atlas [40], exemplary modeling the kidney via a medial representation [35]. Real time animation, while easy to achieve in principle for 3D surface models, poses a challenge for 3D image models. This results from the fact that 3D image warping involves the *inverse* mapping, that is computationally expensive to approximate. An in-depth discussion of that fact is given in Hermann et al. [44] who take advantage of the log-domain framework to compute the inverse.

6. Future challenges

Visual analytics is still a young field and we expect that applying its basic ideas to different applications in visual shape analytics offers the potential for a lot of novel future work. Especially the high potential of visual analytics methods to steer and optimize parameter selection for complex computational models in an interactive way like the segmentaton derived from the covariance analysis for the analysis of shape variation is worthwhile to be investigated in furhter application areas. We believe that some of the presented visual shape analytics techniques could be adapted to investigate the quality of registration and the statistical models themselves. This way parameter settings of the registration algorithm can be optimized which might also improve the resulting statistical shape model this way closing the loop [79]. This reflects a recent trend of applying visual analytics to optimize parameter settings for image segmentation and analysis algorithms, like in [67, 86, 73, 89, 36]. There is a lot more potential to apply some of the already well established techniques to visual shape analytics, e.g. in providing custom linked views to intuitively assess particular extrinsic attributes via a geographic map, a phylogenetic tree or a Manhattan plot for specific genetic analyses. In the future we hope to see more applications of the presented methods in morphometric and computational anatomy studies. Especially population studies provide an ideal application domain because of their exploratory nature [17, 53]. Furthermore, we foresee also novel applications for high-throughput phenotyping of time-varying shape data as nowadays efficient acquisition devices became standard for example in the agricultural domain [32, 31]. In this context there is also potential to apply the outlined methods for part-based models.

From a technical point of view we see several directions for future work. Interactive applications for medial representations [35] for instance would provide another very powerful non-linear statistical model, namely principal geodesic analysis [34]. Another example in this context would be the recent model of Durrleman et al. [29] that describes dense deformations with sparse parameters and can thereby also handle varying topologies, including cases that do not allow a perfect registration. A further challenge are hierarchical shape models that allow investigation of shape variation at multiple scales. There exist several promising approaches utilizing different decompositions of shape variation, either based on wavelet theory [27] (particularly popular in medical image analysis [92, 94, 30]), sparse PCA [78], polyaffine transformation tree [75] or deflation of principal warps [15]. However, effective means of navigating complex multiscale representations have only sparely been addressed so far, partly because the complexity of some of the methods rules out an interactive approach.

7. Conclusion

Visual analytics methods have found application in nearly every domain that requires the analysis of large datasets of high dimensional data, ranging from financial market to climate research. In summary we can state that recent developments in visual shape analytics has proven to be a valuable approach to study shape variability. It requires algorithms for analysis, navigaton and visualization that are capable of interactive performance. So far, such an interactive shape analysis was restricted to landmark and surface models. Using the efficient linear parametrizations of shape variability allows now to operate even on volumetric deformation models describing shape variation at image resolution at interactive rates. This allows us to also consider interior structures and diminutive features that were not accessible to previous landmark and surface based approaches. As shown in this paper the most crucial part of an visual shape analytics system is the interactive navigation in shape space that is assisted by intelligent methods like automatic computation of semantic traits or tailored visualization techniques like covariance tensor glyphs.

Acknowledgements

This work was supported by Deutsche Forschungsgesellschaft within the priority program SPP1335.

References

[1] M. Alexa. Linear combination of transformations. *ACM Trans. Graphics*, 21(3):380–387, 2002.

[2] B. Allen, B. Curless, and Z. Popović. The space of human body shapes: reconstruction and parameterization from range scans. *ACM Trans. Graphics*, pages 587–594, 2003.

[3] D. Anguelov, P. Srinivasan, D. Koller, S. Thrun, J. Rodgers, and J. Davis. SCAPE: shape completion and animation of people. *ACM Trans. Graphics*, 24(3):408–416, 2005.

[4] V. Arsigny, O. Commowick, X. Pennec, and N. Ayache. A log-euclidean framework for statistics on diffeomorphisms. In *Proc. MICCAI*, pages 924–931. Springer, 2006.

[5] J. Ashburner. A fast diffeomorphic image registration algorithm. *NeuroImage*, 38(1):95–113, 2007.

[6] B. Avants and J. C. Gee. Geodesic estimation for large deformation anatomical shape averaging and interpolation. *NeuroImage*, 23:S139–S150, 2004.

[7] A. Bair and D. House. Grid with a view: Optimal texturing for perception of layered surface shape. *IEEE Trans. Visual. Comput. Graphics*, 13(6):1656–1663, nov 2007.

[8] A. H. Barr. Global and local deformations of solid primitives. In *Proc. SIGGRAPH'84*, volume 18, pages 21–30, 1984.

[9] M. F. Beg, M. I. Miller, A. Trouvé, and L. Younes. Computing large deformation metric mappings via geodesic flows of diffeomorphisms. *International Journal of Computer Vision*, 61(2):139–157, 2005.

[10] A. Berner, O. Burghard, M. Wand, N. J. Mitra, R. Klein, and H.-P. Seidel. A morphable part model for shape manipulation. Technical Report MPI-I-2011-4-005, MPI Informatik, Dec. 2011.

[11] J. Blaas, C. P. Botha, and F. H. Post. Interactive visualization of multifield medical data using linked physical and feature-space views. In *Proc. Eurographics/IEEE VGTC Conf. Visualization*, pages 123–130, 2007.

[12] V. Blanz, A. Mehl, T. Vetter, and H.-P. Seidel. A statistical method for robust 3D surface reconstruction from sparse data. In *Proceedings of the 2nd International Symposium on 3D Data Processing Visualization and Transmission (3DPVT'04)*, pages 293–300. IEEE, 2004.

[13] V. Blanz and T. Vetter. A morphable model for the synthesis of 3D faces. In *ACM Trans. Graphics*, pages 187–194, 1999.

[14] F. L. Bookstein. Principal warps: Thin-plate splines and the decomposition of deformations. *IEEE Trans. Pattern Analysis and Machine Intelligence*, 11(6):567–585, 1989.

[15] F. L. Bookstein. Integration, disintegration, and self-similarity: Characterizing the scales of shape variation in landmark data. *Evolutionary Biology*, pages 1–32, 2015.

[16] M. Bossa, M. Hernandez, and S. Olmos. Contributions to 3D diffeomorphic atlas estimation: application to brain images. In *Proc. MICCAI*, pages 667–674. Springer, 2007.

[17] C. P. Botha, B. Preim, A. Kaufman, S. Takahashi, and A. Ynnerman. From individual to population: Challenges in medical visualization. In *Scientific Visualization*, pages 265–282. Springer, 2014.

[18] C. Bregler, A. Hertzmann, and H. Biermann. Recovering non-rigid 3d shape from image streams. *IEEE Computer Vision and Pattern Recognition*, 2:690–696, 2000.

[19] S. Busking, C. P. Botha, and F. H. Post. Direct visualization of deformation in volumes. *Computer Graphics Forum*, 28(3):799–806, 2009.

[20] S. Busking, C. P. Botha, and F. H. Post. Dynamic multi-view exploration of shape spaces. *Computer Graphics Forum*, 29(3):973–982, 2010.

[21] J. J. Caban, P. Rheingans, and T. Yoo. An evaluation of visualization techniques to illustrate statistical deformation models. *Computer Graphics Forum*, 30(3):821–830, 2011.

[22] T. J. Cashman and K. Hormann. A continuous, editable representation for deforming mesh sequences with separate signals for time, pose and shape. *Computer Graphics Forum*, 31:735–744, 2012.

[23] A. Cedilnik and P. Rheingans. Procedural annotation of uncertain information. In *Proc. IEEE Visualization*, pages 77–83, 2000.

[24] G. Christensen, R. Rabbitt, and M. Miller. Deformable templates using large deformation kinematics. *IEEE Trans. Image Processing*, 5(10):1435–1447, Oct. 1996.

[25] D. Coffey, C.-L. Lin, A. G. Erdman, and D. F. Keefe. Design by dragging: An interface for creative forward and inverse design with simulation ensembles. *IEEE Trans. Vis. & Comp. Graphics*, 19(12):2783–2791, 2013.

[26] T. F. Cootes, C. J. Taylor, D. H. Cooper, and J. Graham. Active shape models: Their training and application. *Computer Vision and Image Understanding*, 61(1):38–59, Jan. 1995.

[27] C. Davatzikos, X. Tao, and D. Shen. Hierarchical active shape models, using the wavelet transform. *IEEE Trans. Med. Img.*, 22(3):414–423, 2003.

[28] R. Davies, C. Twining, and C. Taylor. *Statistical models of shape: Optimisation and evaluation*. Springer, 2008.

[29] S. Durrleman, M. Prastawa, N. Charon, J. R. Korenberg, S. Joshi, G. Gerig, and A. Trouvé. Morphometry of anatomical shape complexes with dense deformations and sparse parameters. *NeuroImage*, 101:35–49, 2014.

[30] S. Essafi, G. Langs, and N. Paragios. Hierarchical 3d diffusion wavelet shape priors. In *Proc. IEEE International Conference on Computer Vision*, pages 1717–1724, 2009.

[31] N. Fahlgren, M. A. Gehan, and I. Baxter. Lights, camera, action: high-throughput plant phenotyping is ready for a close-up. *Current opinion in plant biology*, 24:93–99, 2015.

[32] F. Fiorani and U. Schurr. Future scenarios for plant phenotyping. *Annual review of plant biology*, 64:267–291, 2013.

[33] B. Fischer and J. Modersitzki. A unified approach to fast image registration and a new curvature based registration technique. *Linear Algebra and its applications*, 380:107–124, 2004.

[34] P. T. Fletcher, C. Lu, S. M. Pizer, and S. Joshi. Principal geodesic analysis for the study of nonlinear statistics of shape. *IEEE Trans. Medical Imaging*, 23(8):995–1005, 2004.

[35] P. T. Fletcher, S. M. Pizer, A. Thall, and A. G. Gash. Shape modeling and image visualization in 3D with m-rep object models. Technical report, University of North Carolina at Chapel Hill, 2000.

[36] A. Geurts, G. Sakas, A. Kuijper, M. Becker, and T. von Landesberger. Visual comparison of 3d medical image segmentation algorithms based on statistical shape models. Los Angeles, USA, August 2015 2015.

[37] J. Gower. Generalized procrustes analysis. *Psychometrika*, 40:33–51, 1975.

[38] A. Guimond, J. Meunier, and J.-P. Thirion. Average brain models: A convergence study. *Comp. Vis. and Img. UndRst&.*, 77(2):192–210, 2000.

[39] G. Hamarneh, A. D. Ward, and R. Frank. Quantification and visualization of localized and intuitive shape variability using a novel medial-based shape representation. In *Proc. IEEE Symp. Biomedical Imaging (ISBI).*, pages 1232–1235, 2007.

[40] H. Handels and S. Hacker. A framework for representation and visualization of 3D shape variability of organs in an interactive anatomical atlas. *Methods of Information in Medicine*, 48(3):272–281, 2009.

[41] T. Heimann and H.-P. Meinzer. Statistical shape models for 3D medical image segmentation: A review. *Med. Img. Anal.*, 13(4):543 – 563, 2009.

[42] M. Hermann, A. C. Schunke, and R. Klein. Semantically steered visual analysis of highly detailed morphometric shape spaces. In *Proc. IEEE Symp. Biological Data Visualization*, pages 151–158, 2011.

[43] M. Hermann, A. C. Schunke, T. Schultz, and R. Klein. A visual analytics approach to study anatomic covariation. In *Proc. IEEE Pacific Visualization Symp.*, 2014.

[44] M. Hermann, A. C. Schunke, T. Schultz, and R. Klein. Accurate interactive visualization of large deformations and variability in biomedical image ensembles. *IEEE TVCG*, 22(1), 2016. (to appear).

[45] F. Jiao, J. M. Phillips, Y. Gur, and C. R. Johnson. Uncertainty visual-

ization in HARDI based on ensembles of ODFs. In *Proc. IEEE Pacific Visualization Symposium*, pages 193–200, 2012.

[46] S. Joshi, B. Davis, M. Jomier, and G. Gerig. Unbiased diffeomorphic atlas construction for comput. anatomy. *NeuroImage*, 23:151–160, 2004.

[47] D. Keim, J. Kohlhammer, G. Ellis, and F. Mansmann, editors. *Mastering the information age: solving problems with visual analytics*. Eurographics Association, 2010.

[48] D. G. Kendall. The diffusion of shape. *Advances in applied probability*, pages 428–430, 1977.

[49] M. Kilian, N. J. Mitra, and H. Pottmann. Geometric modeling in shape space. *ACM Trans. Graphics*, 26(3):64, 2007.

[50] G. Kindlmann, D. Weinstein, A. Lee, A. Toga, and P. Thompson. Visualization of anatomic covariance tensor fields. *Engineering in Medicine and Biology Society.*, 1:1842–1845, Sept. 2004.

[51] M. Kirschner and S. Wesarg. Interactive visualization of statistical shape models. Poster presentation at Eurographics Workshop on Visual Computing for Biology and Medicine, 2010.

[52] M. Kirschner and S. Wesarg. Active shape models unleashed. *Progress in biomedical optics and imaging*, 12(31), 2011.

[53] P. Klemm, S. Oeltze-Jafra, K. Lawonn, K. Hegenscheid, H. Volzke, and B. Preim. Interactive visual analysis of image-centric cohort study data. *IEEE Trans. Vis. & Comp. Graphics*, pages 1673–1682, 2014.

[54] C. P. Klingenberg. Morphological integration and developmental modularity. *Annu. Rev. Ecol. Evol. Syst.*, pages 115–132, 2008.

[55] C. P. Klingenberg. Cranial integration and modularity: insights into evolution and development from morphometric data. *Hystrix, the Italian Journal of Mammalogy*, 24(1):43–58, 2013.

[56] C. P. Klingenberg. Visualizations in geometric morphometrics: how to read and how to make graphs showing shape changes. *Hystrix, the Italian Journal of Mammalogy*, 24(1):15–24, 2013.

[57] B. Kondo and C. Collins. Dimpvis: Exploring time-varying information visualizations by direct manipulation. *IEEE Trans. Visualization & Computer Graphics*, 20(12):2003–2012, Dec 2014.

[58] H. Lamecker, M. Seebaß, T. Lange, H.-C. Hege, and P. Deuflhard. Visualization of the variability of 3D statistical shape models by animation. *Studies in health technology and informatics*, pages 190–196, 2004.

[59] J. Lewis and K.-i. Anjyo. Direct manipulation blendshapes. *IEEE Computer Graphics and Applications*, 30(4):42 –50, 2010.

[60] M. Lüthi, T. Albrecht, and T. Vetter. Probabilistic modeling and visualization of the flexibility in morphable models. In *Mathematics of Surfaces XIII*, pages 251–264. Springer, 2009.

[61] M. M. Malik, C. Heinzl, and M. E. Groeller. Comparative visualization for parameter studies of dataset series. *IEEE Trans. Visualization & Computer Graphics*, 16(5):829–840, 2010.

[62] W. Matusik, H. Pfister, M. Brand, and L. McMillan. A data-driven reflectance model. *ACM Trans. Graphics*, 22(3):759–769, 2003.

[63] M. I. Miller, A. Trouvé, and L. Younes. On the metrics and euler-lagrange equations of computational anatomy. *Annual review of biomedical engineering*, 4(1):375–405, 2002.

[64] M. I. Miller, A. Trouvé, and L. Younes. Geodesic shooting for computational anatomy. *J. of math. imaging and vision*, 24(2):209–228, 2006.

[65] J. Modersitzki. *Numerical methods for image registration*. Oxf. Univ. Press, 2004.

[66] T. Pfaffelmoser, M. Reitinger, and R. Westermann. Visualizing the positional and geometrical variability of isosurfaces in uncertain scalar fields. In *Computer Graphics Forum*, volume 30, pages 951–960, 2011.

[67] H. Piringer, W. Berger, and J. Krasser. Hypermoval: Interactive visual validation of regression models for real-time simulation. *Computer Graphics Forum*, 29(3):983–992, 2010.

[68] K. Pöthkow and H.-C. Hege. Positional uncertainty of isocontours: Condition analysis and probabilistic measures. *IEEE Trans. Visualization & Computer Graphics*, 17(10):1393–1406, 2011.

[69] A. Reh, C. Gusenbauer, J. Kastner, M. E. Groller, and C. Heinzl. Mobjects–a novel method for the visualization and interactive exploration of defects in industrial xct data. *IEEE Trans. Visualization & Computer Graphics*, 19(12):2906–2915, 2013.

[70] W. R. Riddle, R. Li, J. M. Fitzpatrick, S. C. DonLevy, B. M. Dawant, and R. R. Price. Characterizing changes in MR images with color-coded Jacobians. *Magnetic resonance imaging*, 22(6):769–777, 2004.

[71] D. Rueckert, A. F. Frangi, and J. A. Schnabel. Automatic construction of 3D statistical deformation models using non-rigid registration. In *Proc. MICCAI*, pages 77–84. Springer, 2001.

[72] G. Sakas and M. Gerth. Sampling and anti-aliasing of discrete 3-d volume density textures. *Computers & Graphics*, 16(1):121–134, 1992.

[73] T. Schultz and G. Kindlmann. Open-box spectral clustering: Applications to medical image analysis. *IEEE Trans. Visualization & Computer Graphics*, 19(12):2100–2108, 2013.

[74] T. W. Sederberg and S. R. Parry. Free-form deformation of solid geometric models. In *Proceedings of SIGGRAPH'86*, pages 151–160, 1986.

[75] C. Seiler, X. Pennec, and M. Reyes. Capturing the multiscale anatomical shape variability with polyaffine transformation trees. *Medical Image Analysis*, 16(7):1371 – 1384, 2012.

[76] C. Seiler, X. Pennec, L. Ritacco, and M. Reyes. Femur specific polyaffine model to regularize the log-domain demons registration. In *Proc. SPIE Medical Imaging*, volume 7962, Mar. 2011.

[77] B. Shneiderman. The eyes have it: a task by data type taxonomy for information visualizations. In *Proc. IEEE Symp. Visual Languages*, pages 336–343, 1996.

[78] K. Sjöstrand, M. B. Stegmann, and R. Larsen. Sparse principal component analysis in medical shape modeling. In J. M. Reinhardt and J. P. W. Pluim, editors, *Proc. SPIE Medical Imaging*, volume 6144, Mar. 2006.

[79] N. N. Smit, B. Klein Haneveld, M. Staring, E. Eisemann, C. P. Botha, and A. Vilanova. RegistrationShop: An interactive 3D medical volume registration system. In *Eurographics Workshop on Visual Computing for Biology and Medicine (VCBM)*, pages 145–153, 2014.

[80] R. Smith, R. Pawlicki, I. Kokai, J. Finger, and T. Vetter. Navigating in a shape space of registered models. *IEEE Trans. Visualization & Computer Graphics*, 13(6):1552–1559, 2007.

[81] A. Sotiras, C. Davatzikos, and N. Paragios. Deformable medical image registration: A survey. *IEEE Trans. Med. Img.*, 32(7):1153–1190, 2013.

[82] J. R. Tena, F. De la Torre, and I. Matthews. Interactive region-based linear 3D face models. *ACM Trans. Graphics*, 30:76:1–76:10, 2011.

[83] D. W. Thompson. *On Growth and Form: A New Edition*. Cambridge University Press, 1942.

[84] P. M. Thompson and A. W. Toga. Detection, visualization and animation of abnormal anatomic structure with a deformable probabilistic brain atlas based on random vector field transformations. *Medical image analysis*, 1(4):271–294, 1997.

[85] M. Tittgemeyer, G. Wollny, and F. Kruggel. Visualising deformation fields computed by non-linear image registration. *Computing and Visualization in Science*, 5(1):45–51, 2002.

[86] T. Torsney-Weir, A. Saad, T. Möller, H.-C. Hege, B. Weber, and J.-M. Verbavatz. Tuner: Principled parameter finding for image segmentation algorithms using visual response surface exploration. *IEEE Trans. Visualization & Computer Graphics*, 17(12):1892–1901, 2011.

[87] E. R. Tufte. *Envisioning information*. Graphics Press, 1990.

[88] K. Van Golen. Landmark influence visualization in active shape models. Master's thesis, TU Delft, Delft University of Technology, 2014.

[89] T. von Landesberger, G. Andrienko, N. Andrienko, S. Bremm, M. Kirschner, S. Wesarg, and A. Kuijper. Opening up the "black box" of medical image segmentation with statistical shape models. *The Visual Computer*, 29(9):893–905, 2013.

[90] G. Wahba. *Spline models for observational data*. Siam, 1990.

[91] D. F. Wiley, N. Amenta, D. A. Alcantara, D. Ghosh, Y. J. Kil, E. Delson, W. Harcourt-Smith, K. S. John, F. J. Rohlf, and B. Hamann. Evolutionary morphing. In *Proc. IEEE Visualization*, pages 431–438, 2005.

[92] Z. Xue, D. Shen, and C. Davatzikos. Statistical representation of high-dimensional deformation fields with application to statistically constrained 3d warping. *Medical Image Analysis*, 10(5):740–751, 2006.

[93] A. J. Yezzi and S. Soatto. Deformotion: Deforming motion, shape average and the joint registration and approximation of structures in images. *Int. Journal of Computer Vision*, 53(2):153–167, 2003.

[94] P. Yu, P. E. Grant, Y. Qi, X. Han, F. Ségonne, R. Pienaar, E. Busa, J. Pacheco, N. Makris, R. L. Buckner, et al. Cortical surface shape analysis based on spherical wavelets. *IEEE Trans. Medical Imaging*, 26(4):582–597, 2007.

[95] C. Zhang, T. Schultz, K. Lawonn, E. Eisemann, and A. Vilanova. Glyph-based comparative visualization for diffusion tensor fields. *IEEE Trans. Visualization & Computer Graphics*, 22(1), 2016.

[96] C. P. E. Zollikofer and M. S. Ponce De Léon. Visualizing patterns of craniofacial shape variation in *Homo sapiens*. In *Biological Sciences 269(1493)*, pages 801–807, 2002.